Automatica 123 (2021) 109294

Contents lists available at ScienceDirect

Automatica

journal homepage: www.elsevier.com/locate/automatica

Shared control for switched motorized FES-cycling on a split-crank cycle accounting for muscle control input saturation ☆

Courtney A. Rouse *, Christian A. Cousin, Brendon C. Allen, Warren E. Dixon

Department of Mechanical and Aerospace Engineering, University of Florida, Gainesville, USA

ARTICLE INFO

Article history:
Received 25 April 2019
Received in revised form 27 May 2019
Accepted 11 September 2019
Available online 2 November 2020

ABSTRACT

Closed-loop functional electrical stimulation (FES) control methods are developed to enable motorized assistive split-crank (i.e., a cycle without mechanical coupling between the lower limbs) cycling for rehabilitation efforts for people with lower limb movement disorders. The non-dominant side tracks a desired range of cadence and the dominant side tracks a range of position offsets centered around the position of the non-dominant side. A multi-level switched system with switched control objectives is applied to both sides of the cycle-rider system. Assistive, uncontrolled, and resistive modes for the dominant and non-dominant subsystems are based on position and cadence, respectively. Global exponential tracking to upper and lower bounds of an uncontrolled desired region is proven for each side via Lyapunov-based analysis using switched system methods. Experiments on both able-bodied participants and participants with neuromuscular conditions show the performance of the switched control system for split-crank FES-cycling. From volitional to controlled pedaling in able-bodied participants, average RMS cadence error of the non-dominant, RMS position error of the dominant, and cadence differential between the two legs improved by 76.2%, 65.3%, and 58.0%, respectively. On average, experiments on participants with neuromuscular conditions resulted in RMS errors that were 45.8%, 92.6%, and 52.0% higher than controlled trials on able-bodied participants, but 65.3%, 33.3%, and 36.3% lower than volitional-only trials of able-bodied participants.

1. Introduction

Functional electrical stimulation (FES) cycling is a commonly used rehabilitation exercise for people with neuromuscular conditions that result in movement disorders (Ambrosini, Ferrante, Pedrocchi, Ferrigno, & Molteni, 2011; Ferrante, Pedrocchi, Ferrigno, & Molteni, 2008; Hooker et al., 1992; Janssen et al., 2008; Johnston, Smith, Oladeji, Betz, & Lauer, 2008; Kuhn, Leichtfried, & Schobersberger, 2014; Sadowsky et al., 2013). For some conditions, one side of the body is affected more than the other (i.e., hemiparesis). When a person with hemiparesis pedals a traditional single-crank cycle, their dominant side can mask the weakness in their impaired side due to the pedal coupling at the crank. While their tracking goals may be met (e.g., pedaling at a desired cadence), challenging the impaired side may improve hemiparesis and avoid creating a larger gap in their existing bilateral asymmetry. Thus, cycling for rehabilitation of movement disorders involving hemiparesis should promote equal contribution from the dominant and impaired limbs (Chen, Chen, Chen, Fu, & Wang, 2005). To reduce muscular asymmetries, some studies have tasked controllers with balancing torques on either side of a single-crank FES-cycle (Ambrosini, Ferrante, Ferrigno, Molteni, & Pedrocchi, 2012; Ambrosini et al., 2011, 2014), while other cycling studies have used split-crank cycles to address muscular asymmetries (Estay, Rouse, Cohen, Cousin, & Dixon, 2019; Van der Loos, Worthen-Chaudhari, & Schwandt, 2010; Rouse, Cousin, Allen, & Dixon, 2019; Ting, Kautz, Brown, Van der Loos, & Zajac, 1998; Ting, Kautz, Brown, & Zajac, 2000; Ting, Raasch, Brown, Kautz, & Zajac, 1998), as in the current result. However, only Estay et al. (2019), Rouse et al. (2019) and Van der Loos et al. (2010) have focused on closed-loop control of the cycle-rider system, and aside from our prolegomenous work in Estay et al. (2019) and Rouse et al. (2019), no previous split-crank cycling studies have used FES to control the rider's muscles.

Because physical therapy participants vary in their strength and abilities, it is important to establish rehabilitation exercise protocols that can be broadly applied, where volitional contributions are encouraged for active therapy (Hogan et al., 2006). Moreover, volitional contribution combined with electrical stimulation has been shown to enhance functional improvements

☆ The material in this paper was partially presented at the 2019 American Control Conference (ACC), July 10–12, 2019, Philadelphia, PA, USA. This paper was recommended for publication in revised form by Associate Editor Antonella Ferrara under the direction of Editor Thomas Parisini.

* Corresponding author.
E-mail addresses: courtneyarouse@ufl.edu (C.A. Rouse), ccousin@ufl.edu (C.A. Cousin), brendoncallen@ufl.edu (B.C. Allen), wdixon@ufl.edu (W.E. Dixon).

https://doi.org/10.1016/j.automatica.2020.109294

(Iyanaga et al., 2019; Kraft, Fitts, & Hammond, 1992). Some participants may benefit from using volitional control to follow a trajectory range, rather than a precise trajectory or performance specification (Asl, Narikiyo, & Kawanishi, 2017; Hogan et al., 2006). A trajectory range can be tracked using assist-as-needed controllers, such as those in many rehabilitation robots (Asl et al., 2017; Banala, Kim, Agrawal, & Scholz, 2009; Cousin, Duenas, Rouse, & Dixon, 2018; Duschau-Wicke, von Zitzewitz, Caprez, Lunenburger, & Riener, 2010; Pehlivan, Losey, & O'Malley, 2016; Srivastava et al., 2015, 2016). In Rouse, Cousin, Duenas, and Dixon (2018), a novel closed-loop state-dependent switched system strategy was developed to assist volitionally pedaling participants when they pedal below a minimum desired cadence and resist them when they exceed the maximum desired cadence. As the person pedals, the switched system automatically transitions between assistive, uncontrolled, and resistive modes according to minimum and maximum cadence bounds. The work in Rouse et al. (2019) implements a similar strategy on a split-crank cycle to benefit a broad range of strength, ability, and hemiparesis.

While FES-cycling is a long-standing topic of research, most research has ignored limitations of the participant such as the need to saturate the stimulation input based on comfort levels and safety. In FES-cycling, motor control is often implemented in regions of the crank cycle where muscles do not efficiently produce torque (Bellman, Downey, Parikh, & Dixon, 2017); however, in this paper, the motors (one for each side of the split-crank cycle) also assist in FES regions as needed when the FES control input saturates at the comfort threshold, similar to the protocol developed in Rouse, Cousin, Duenas, and Dixon (2017) for FES biceps curls.

As in Rouse et al. (2019) and Rouse et al. (2018), this paper implements arbitrary and state-dependent switching between and within three modes (i.e., assistive, uncontrolled, and resistive) as the continuous state-dynamics evolve. High-level switching denotes switching amongst the three modes and is based on cadence and position for the non-dominant and dominant sides, respectively. Mid-level position-dependent switching within the assistive mode of each side occurs between the quadriceps, gluteal, and hamstring muscle groups, and the electric motor, similar to results such as Bellman et al. (2017). Low-level switching denotes the arbitrary switching within FES regions of the assistive mode to distribute partial control authority to the motor whenever the FES control input to a muscle saturates. Like the preliminary work in Rouse et al. (2019), which also utilized a split-crank cycle, the non-dominant side is resisted by an electric motor when pedaling above the desired cadence region and assisted via a combination of FES and the electric motor when below the desired cadence region. Similarly, the dominant leg is appropriately assisted or resisted when its position is outside a desired range centered at 180 degrees out of phase from the non-dominant leg. This paper improves upon the preliminary work by using comfort thresholds individually selected for each muscle group. Separate saturation limits on each individual muscle control input necessitate a change in the stability analysis to account for the saturation of some muscle groups but not others. Moreover, the motor controller design is updated to better distribute control authority when a muscle group reaches its comfort threshold. Aside from the additional theoretical contribution, the current work also provides experimental results from three people with neurological conditions and three able-bodied participants.

Without the gravitational force of one leg affecting the motion of the opposite leg (as in traditional cycling), a split-crank cycle is much more difficult to pedal than a single-crank cycle. To show the benefit of the controller, able-bodied participants were asked to perform two trials with volitional contribution, one with and one without FES activation or the motors. While the control design is motivated by issues involving hemiparesis, the subsequently developed protocol is also applicable to people with symmetric limb control, in which case the dominant side may be selected arbitrarily.

The remainder of this paper includes a nonlinear dynamic model of the cycle-rider system in Section 2, control development in Section 3, stability analysis in Section 4, and experimental results in Section 5. For the cycle-rider system, position-based, cadence-based, and arbitrary switching occurs, and the dominant and impaired cases must be analyzed separately. Switching between stable subsystems can result in instability (Liberzon, 2003); hence the switched system analysis employs a common Lyapunov function candidate with a set valued generalized derivative to prove global exponential stability in the assistive and resistive modes. Experimental results depict all three cycling modes and demonstrate the performance of the developed controller for people with varied abilities. On average, RMS cadence errors of the non-dominant sides improved by 76.2% from volitional to controlled trials in able-bodied participants, while RMS position errors of the dominant side improved by 65.3% and cadence differentials between the two legs improved by 58.0%, on average. Experiments on participants with neuromuscular conditions resulted in average RMS cadence and position errors and average RMS cadence differentials that were 45.8%, 92.6%, and 52.0% higher, respectively, than controlled trials on able-bodied participants, but 65.3%, 33.3%, and 36.3% lower than volitional-only trials of able-bodied participants.

2. Model

The switched dynamics of the cycle-rider system are considered separately for both sides and are derived in Rouse et al. (2019) as[1]

$$\sum_{m\in\mathcal{M}} B_m u_{m_l} + B_{e_l} u_{e_l} + \tau_{vol_l} = M_l\ddot{q}_l + b_{c_l}\dot{q}_l + d_{c_l} + V_l\dot{q}_l + G_l + P_l + d_{r_l}, \tag{1}$$

$\forall l \in S \triangleq \{1, 2\}$, which indicates the impaired/non-dominant ($l = 1$) and dominant ($l = 2$) sides, respectively, and $m \in \mathcal{M} \triangleq \{Q, G, H\}$ indicates the quadriceps femoris (Q), gluteal (G), and hamstring (H) muscle groups, respectively. The measurable crank angle is denoted by $q_l : \mathbb{R}_{\geq 0} \to \mathcal{Q}$, where $\mathcal{Q} \subseteq \mathbb{R}$ is the set of all possible crank angles. The measurable crank velocity is denoted by $\dot{q}_l : \mathbb{R}_{\geq 0} \to \mathbb{R}$, and the unmeasured acceleration is denoted by $\ddot{q}_l : \mathbb{R}_{\geq 0} \to \mathbb{R}$. The uncertain muscle control effectiveness is denoted by $B_m : \mathcal{Q} \times \mathbb{R} \to \mathbb{R}_{>0}$, as in Bellman et al. (2017) and Idsø, Johansen, and Hunt (2004); $u_{m_l} : \mathbb{R}_{\geq 0} \to \mathbb{R}$ denotes the FES stimulation intensity (i.e., pulse width); the motor control constant is denoted by $B_{e_l} \in \mathbb{R}_{>0}$ and relates the motor's input current to output torque; and $u_{e_l} : \mathbb{R}_{\geq 0} \to \mathbb{R}$ denotes the subsequently designed motor control input. Torques produced by the participant's volition are denoted by τ_{vol_l}. Combined inertial effects of the cycle and rider are denoted by $M_l : \mathcal{Q} \to \mathbb{R}$; $b_{c_l} \in \mathbb{R}_{>0}$ and $d_{c_l} : \mathbb{R}_{\geq 0} \to \mathbb{R}$, denote viscous damping effects and disturbances applied by the cycle, respectively; $V_l : \mathcal{Q} \times \mathbb{R} \to \mathbb{R}$, $G_l : \mathcal{Q} \to \mathbb{R}$, $P_l : \mathcal{Q} \times \mathbb{R} \to \mathbb{R}$, and $d_{r_l} : \mathbb{R}_{\geq 0} \to \mathbb{R}$ denote the effects of centripetal–Coriolis, gravitational, passive viscoelastic tissue forces, and rider disturbances, respectively.

High-level switching occurs on both sides of the cycle (i.e., $\forall l \in S$) between assistive, uncontrolled, and resistive modes according

[1] For notational brevity, all functional dependencies are suppressed unless required for clarity of exposition.

to the subsequently designed switching signals. On the non-dominant side, the velocity- (i.e., cadence-) based high-level switching laws are defined as

$$\sigma_{a_1} \triangleq \begin{cases} 1 & \text{if} \quad \dot{q}_1 \leq \dot{q}_{\underline{d}1} \\ 0 & \text{if} \quad \dot{q}_1 > \dot{q}_{\underline{d}1} \end{cases}, \quad \sigma_{r_1} \triangleq \begin{cases} 1 & \text{if} \quad \dot{q}_1 \geq \dot{q}_{\bar{d}1} \\ 0 & \text{if} \quad \dot{q}_1 < \dot{q}_{\bar{d}1} \end{cases}, \tag{2}$$

where the switching signals $\sigma_{a_1} : \mathbb{R} \to \{0, 1\}$ and $\sigma_{r_1} : \mathbb{R} \to \{0, 1\}$ define the assistive (i.e., $\sigma_{a_1} = 1$, $\sigma_{r_1} = 0$) and resistive (i.e., $\sigma_{a_1} = 0$, $\sigma_{r_1} = 1$) modes, respectively. The switching point between the assistive and uncontrolled (i.e., $\sigma_{a_1} = 0$, $\sigma_{r_1} = 0$) modes is denoted by $\dot{q}_{\underline{d}1} : \mathbb{R}_{\geq 0} \to \mathbb{R}$, which represents the selectable minimum desired cadence value. The switching point between the uncontrolled and resistive modes is denoted by $\dot{q}_{\bar{d}1} : \mathbb{R}_{\geq 0} \to \mathbb{R}$ and represents the selectable maximum desired cadence value. Thus, the uncontrolled mode for the non-dominant side is active when $\dot{q}_1 \in \left[\dot{q}_{\underline{d}1}, \dot{q}_{\bar{d}1}\right]$. Similarly, high-level switching between the three modes (i.e., assistive, resistive, and uncontrolled) on the dominant side is based on position, such that

$$\sigma_{a_2} \triangleq \begin{cases} 1 & \text{if} \quad q_2 \leq q_{\underline{d}2} \\ 0 & \text{if} \quad q_2 > q_{\underline{d}2} \end{cases}, \quad \sigma_{r_2} \triangleq \begin{cases} 1 & \text{if} \quad q_2 \geq q_{\bar{d}2} \\ 0 & \text{if} \quad q_2 < q_{\bar{d}2} \end{cases}, \tag{3}$$

where the switching signals $\sigma_{a_2} : \mathcal{Q} \to \{0, 1\}$ and $\sigma_{r_2} : \mathcal{Q} \to \{0, 1\}$ define the assistive (i.e., $\sigma_{a_2} = 1$, $\sigma_{r_2} = 0$) and resistive (i.e., $\sigma_{a_2} = 1$, $\sigma_{r_2} = 0$) modes for the dominant side, respectively. The dominant side is designed to track the non-dominant side's position such that the switching points between the uncontrolled (i.e., $\sigma_{a_2} = 0$, $\sigma_{r_2} = 0$) mode and the assistive and resistive modes are denoted by $q_{\underline{d}2} : \mathbb{R}_{\geq 0} \to \mathbb{R}$ and $q_{\bar{d}2} : \mathbb{R}_{\geq 0} \to \mathbb{R}$, respectively, and defined as $q_{\underline{d}2} \triangleq q_1 - \pi - \Delta_{d2}$ and $q_{\bar{d}2} \triangleq q_1 - \pi + \Delta_{d2}$, where $\Delta_{d2} \in \mathbb{R}_{>0}$ is the range of allowable position values for the dominant leg to deviate from the non-dominant side. Thus, $q_{\underline{d}2}$ and $q_{\bar{d}2}$ are the selectable minimum and maximum desired position values that bound the dominant side's uncontrolled mode, and are centered around $q_1 - \pi$ to maintain a 180 degree offset[2]. Each subsystem is in its respective uncontrolled mode when $\sigma_{a_l} = \sigma_{r_l} = 0$, $\forall l \in S$. Within the assistive mode for both the non-dominant and dominant subsystems, low-level switching amongst the muscle groups and motor is based on definitions for the subsequent FES regions for each muscle group $\mathcal{Q}_m \subset \mathcal{Q}$, $\forall m \in \mathcal{M}$, as in Rouse et al. (2018). A schematic of the three levels of switching is also included in Fig. 1 of Rouse et al. (2018). The stimulation intensity applied to each muscle group u_{m_l} is defined as

$$u_{m_l} \triangleq \sigma_{a_l}\sigma_{m_l}\text{sat}_{\beta_{m_l}}\left[k_{m_l}u_{s_l}\right], \tag{4}$$

$\forall l \in S$, $\forall m \in \mathcal{M}$, where σ_{a_l} was defined in (2) and (3), the subsequently designed FES control input is denoted by $u_{s_l} : \mathbb{R}_{\geq 0} \to \mathbb{R}$, and $k_{m_l} \in \mathbb{R}_{>0}$ is a selectable constant control gain. The saturation function $\text{sat}_{\beta_{m_l}}(\cdot)$ is defined as $\text{sat}_{\beta_{m_l}}(\kappa) \triangleq \kappa$ for $|\kappa| \leq \beta_{m_l}$ and $\text{sat}_{\beta_{m_l}}(\kappa) \triangleq \text{sgn}(\kappa)\beta_{m_l}$ for $|\kappa| > \beta_{m_l}$, where $\beta_{m_l} \in \mathbb{R}_{>0}$ is the user-defined comfort threshold for each muscle group on each side. The low-level switching signal $\sigma_{m_l} : \mathcal{Q} \to \{0, 1\}$ is designed for each muscle group such that $\sigma_{m_l}(q_l) = 1$ when $q_l \in \mathcal{Q}_m$ and $\sigma_{m_l}(q_l) = 0$ when $q_l(t) \notin \mathcal{Q}_m$, $\forall l \in S$, $\forall m \in \mathcal{M}$. The overall FES region, $\mathcal{Q}_{FES}$, is identical for each side and defined as the union of individual muscle regions, i.e., $\mathcal{Q}_{FES} \triangleq \bigcup_{m \in \mathcal{M}} \{\mathcal{Q}_m\}$, $\forall m \in \mathcal{M}$.

The applied motor current u_{e_l} is defined as

$$u_{e_l} \triangleq \left(\sigma_{r_l} + \sigma_{a_l}\sigma_{e_l}\right) u_{r_l}, \tag{5}$$

$\forall l \in S$, where $u_{r_l} : \mathbb{R}_{\geq 0} \to \mathbb{R}$ denotes the subsequently designed motor control input, and $\sigma_{e_l} : \mathcal{Q} \times \mathbb{R}_{\geq 0} \to (0, 1)$ is an auxiliary switching signal corresponding to mid- and low-level switching for activation of the electric motor within the assistive mode, defined as

$$\sigma_{e_l} \triangleq \begin{cases} 1 & \text{if} \quad q_l \notin \mathcal{Q}_{FES} \\ \gamma_l & \text{if} \quad q_l \in \mathcal{Q}_{FES},\ u_{m_l} = \beta_{m_l} \\ 0 & \text{if} \quad q_l \in \mathcal{Q}_{FES},\ u_{m_l} \neq \beta_{m_l} \end{cases}, \tag{6}$$

$\forall l \in S$, $\forall m \in \mathcal{M}$. Hence, the motor can be activated in the assistive mode in FES and non-FES regions, where $\gamma_l : \mathbb{R}_{\geq 0} \to \mathbb{R}_{\geq 0}$ is the motor's ratio of control authority, defined (based on all muscle control inputs on that side) as the sum $\gamma_l \triangleq \sum_{m \in \mathcal{M}} \frac{k_{m_l}u_{s_l} - \beta_{m_l}}{\beta_{m_l}}$, $\forall l \in S$. When a subsystem is in an FES region, the corresponding motor only activates when the stimulation input for any muscle group within that subsystem/side reaches its respective comfort threshold β_{m_l} and γ_l proportionately distributes the remaining control effort to the motor. Thus, the switching laws autonomously activate subsets of muscle groups and the motor based on position, velocity, and stimulation level.

Substituting (2)–(6) into (1) yields

$$\sum_{m \in \mathcal{M}} B_m \sigma_{a_l}\sigma_{m_l}\text{sat}_{\beta_{m_l}}\left[k_{m_l}u_{s_l}\right] + B_{E_l}u_{r_l} + \tau_{vol_l} = M_l\ddot{q}_l + b_{c_l}\dot{q}_l + d_{c_l} + V_l\dot{q}_l + G_l + P_l + d_{r_l}, \tag{7}$$

$\forall l \in S$, where $B_{E_1} : \mathcal{Q} \times \mathbb{R} \times \mathbb{R}_{\geq 0} \to \mathbb{R}$ and $B_{E_2} : \mathcal{Q} \times \mathbb{R}_{\geq 0} \to \mathbb{R}$ are the switched motor control effectiveness for each side, defined as

$$B_{E_l} \triangleq B_e\left(\sigma_{r_l} + \sigma_{a_l}\sigma_{e_l}\right). \tag{8}$$

The parameters in (7) capture the torques that affect the dynamics of the combined cycle-rider system, but the exact value of these parameters is unknown for each rider and the cycle. However, the subsequently designed FES and motor controllers only require known bounds on the aforementioned parameters. Thus, the switched system in (7) has the following properties and assumption $\forall l \in S$ (Bellman, Cheng, Downey, & Dixon, 2014).

Property 1. *$c_m \leq M_l \leq c_M$, where c_m, $c_M \in \mathbb{R}_{>0}$ are known constants.*

Property 2. *$|V_l| \leq c_V|\dot{q}_l|$, where $c_V \in \mathbb{R}_{>0}$ is a known constant.*

Property 3. *$|G_l| \leq c_G$, where $c_G \in \mathbb{R}_{>0}$ is a known constant.*

Property 4. *$|P_l| \leq c_{P1} + c_{P2}|\dot{q}_l|$, where c_{P1}, $c_{P2} \in \mathbb{R}_{>0}$ are known constants.*

Property 5. *$b_{c_l} \leq c_b$, where $c_b \in \mathbb{R}_{>0}$ is a known constant.*

Property 6. *$|d_{r_l} + d_{c_l}| \leq c_d$, where $c_d \in \mathbb{R}_{>0}$ is a known constant.*

Property 7. *$\frac{1}{2}\dot{M}_l = V_l$.*

Property 8. *B_m is lower bounded $\forall m \in \mathcal{M}$, and thus, when $\sum_{m \in \mathcal{M}} \sigma_{m_l} > 0$, $c_{b_m} \leq B_m \leq c_{b_M}$, $\forall l \in S$, where c_{b_m}, $c_{b_M} \in \mathbb{R}_{>0}$ are known constants.*

Property 9. *$c_{b_e} \leq B_{e_l}$, where $c_{b_e} \in \mathbb{R}_{>0}$ is a known constant.*

Assumption 1. The volitional torque produced by each leg of the rider is bounded due to human physical limitations as $\left|\tau_{vol_l}\right| \leq c_{vol}$, where $c_{vol} \in \mathbb{R}_{>0}$ is a known constant.

3. Control development

The control objective is for the non-dominant subsystem to regulate the cadence to a desired range and for the dominant subsystem to regulate the position to a desired range such that a crank phase difference within a desired range centered at 180 degrees from the dominant leg is maintained.

[2] Definitions for $q_{\underline{d}2}$ and $q_{\bar{d}2}$ represent a shift of π radians; however, this offset could be arbitrarily selected or time-varying.

3.1. Non-dominant side

The cadence tracking objective for the non-dominant leg is quantified by the velocity error $e_1 : \mathbb{R}_{\geq 0} \to \mathbb{R}$ and auxiliary error $r_1 : \mathbb{R}_{\geq 0} \to \mathbb{R}$, defined as

$$e_1 \triangleq \dot{q}_{\underline{d}1} - \dot{q}_1, \tag{9}$$

$$r_1 \triangleq e_1 + \left(1 - \sigma_{a_1}\right) \Delta_{d1}, \tag{10}$$

where $\dot{q}_{\underline{d}1}$, $\dot{q}_{\bar{d}1}$, and Δ_{d1} is defined as $\Delta_{d1} \triangleq \dot{q}_{\bar{d}1} - \dot{q}_{\underline{d}1}$. Taking the time derivative of (9), multiplying by M_1, and using (7) with $l = 1$ yield

$$M_1 \dot{e}_1 = -B_{E_1} u_{r_1} - \tau_{vol_1} - V_1 r_1 + \chi_1 - \sum_{m \in \mathcal{M}} B_m \sigma_{a_1} \sigma_{m_1} \text{sat}_{\beta_{m_1}} \left[k_{m_1} u_{s_1}\right], \tag{11}$$

where the auxiliary term $\chi_1 : \mathcal{Q} \times \mathbb{R} \times \mathbb{R}_{\geq 0} \to \mathbb{R}$ is defined as $\chi_1 \triangleq b_{c_1} \dot{q}_1 + d_{c_1} + G_1 + P_1 + d_{r_1} + V_1 \dot{q}_{\underline{d}1} + V_1 \left(1 - \sigma_{a_1}\right) \Delta_{d1} + M_1 \ddot{q}_{\underline{d}1}$. From Properties 1-6, χ_1 can be bounded as

$$|\chi_1| \leq c_1 + c_2 |e_1|, \tag{12}$$

where $c_1, c_2 \in \mathbb{R}_{>0}$ are known constants, and $|\cdot|$ denotes the absolute value. Based on (11), (12), and the subsequent stability analysis, the FES control input to the muscle groups on the non-dominant side is designed as

$$u_{s_1} = k_{1s} + k_{2s} r_1, \tag{13}$$

where $k_{1s}, k_{2s} \in \mathbb{R}_{>0}$ are constant selectable control gains. The switched control input to the motor is designed as

$$u_{r_1} = k_{1e} \text{sgn}\left(r_1\right) + k_{2e} r_1, \tag{14}$$

where $k_{1e}, k_{2e} \in \mathbb{R}_{>0}$ are constant selectable control gains. Substituting (13) and (14) into (11) yields

$$M_1 \dot{e}_1 = -B_{E_1} \left(k_{1e} \text{sgn}\left(r_1\right) + k_{2e} r_1\right) - \tau_{vol_1} - V_1 r_1 + \chi_1 - \sum_{m \in \mathcal{M}} B_m \sigma_{a_1} \sigma_{m_1} \text{sat}_{\beta_{m_1}} \left[k_{m1} \left(k_{1s} + k_{2s} r_1\right)\right]. \tag{15}$$

3.2. Dominant side

The position tracking objective for the dominant leg is quantified by the error $e_2 : \mathbb{R}_{\geq 0} \to \mathbb{R}$ and auxiliary errors $r_2 : \mathbb{R}_{\geq 0} \to \mathbb{R}$ and $r_3 : \mathbb{R}_{\geq 0} \to \mathbb{R}$, defined as

$$e_2 \triangleq q_{\underline{d}2} - q_2, \tag{16}$$

$$r_2 \triangleq e_2 + (1 - \sigma_{a2}) \Delta_{d2}, \tag{17}$$

$$r_3 \triangleq \dot{e}_2 + \alpha e_2, \tag{18}$$

where $\alpha \in \mathbb{R}_{>0}$ is a constant selectable control gain and $q_{\underline{d}2}$, $q_{\bar{d}2}$, and Δ_{d2} were defined previously. Taking the time derivative of (18), multiplying by M_2, and using (7) with $l = 2$ and (16) yields

$$M_2 \dot{r}_3 = -B_{E_2} u_{r_2} - \tau_{vol_2} - V_2 r_3 - r_2 + \chi_2 - \sum_{m \in \mathcal{M}} B_m \sigma_{a_2} \sigma_{m_2} \text{sat}_{\beta_{m_2}} \left[k_{m_2} u_{s_2}\right], \tag{19}$$

where the auxiliary term $\chi_2 : \mathcal{Q} \times \mathbb{R} \times \mathbb{R}_{\geq 0} \to \mathbb{R}$ is defined as $\chi_2 \triangleq b_{c_2} \dot{q}_2 + d_{c_2} + G_2 + P_2 + d_{r_2} + V_2 \dot{q}_{\underline{d}2} + V_2 \alpha e_2 + M_2 \ddot{q}_{\underline{d}2} + M_2 \alpha r_3 - M_2 \alpha^2 e_2 + r_2$. From Properties 1-6, χ_2 can be bounded as

$$|\chi_2| \leq c_3 + c_4 \|z\| + c_5 \|z\|^2, \tag{20}$$

where $z \triangleq [r_2 \; r_3]^T$, $\|\cdot\|$ is the Euclidean norm, and $c_3, c_4, c_5 \in \mathbb{R}_{>0}$ are known constants. Based on (19), (20), and the subsequent stability analysis, the FES control input to the muscle groups on the dominant side is designed as

$$u_{s_2} = k_{3s} r_3 + \left(k_{4s} + k_{5s} \|z\| + k_{6s} \|z\|^2\right) \text{sgn}\left(r_3\right), \tag{21}$$

where $k_{3s}, k_{4s}, k_{5s}, k_{6s} \in \mathbb{R}_{>0}$ are constant selectable control gains. The switched control input to the motor on the dominant side is designed as

$$u_{r_2} = k_{3e} r_3 + \left(k_{4e} + k_{5e} \|z\| + k_{6e} \|z\|^2\right) \text{sgn}\left(r_3\right), \tag{22}$$

where $k_{3e}, k_{4e}, k_{5e}, k_{6e} \in \mathbb{R}_{>0}$ are constant selectable control gains. Substituting (21) and (22) into (19) yields

$$M_2 \dot{r}_3 = -\sum_{m \in \mathcal{M}} B_m \sigma_{a_2} \sigma_{m_2} \text{sat}_{\beta_{m_2}} \Big[k_{m_2} k_{3s} r_3 + k_{m_2} \left(k_{4s} + k_{5s} \|z\| + k_{6s} \|z\|^2\right) \text{sgn}\left(r_3\right) \Big] - \tau_{vol_2} - V_2 r_3 - r_2 + \chi_2 - B_{E_2} \Big[k_{3e} r_3 + \left(k_{4e} + k_{5e} \|z\| + k_{6e} \|z\|^2\right) \text{sgn}\left(r_3\right) \Big], \tag{23}$$

4. Stability analysis

The stability analysis is divided into non-dominant (Section 4, A) and dominant (Section 4, B) subsystems. To facilitate the analysis of switching signals, switching times are denoted by $\left\{t^i_{n,l}\right\}$, $i \in \{a, r, u\}$, $n \in \{0, 1, 2, \ldots\}$, $\forall l \in S$, representing the times when each side's subsystem switches into the assistive ($i = a$), resistive ($i = r$), or uncontrolled ($i = u$) modes (i.e., every time a switch occurs, $n^+ = n + 1$).

4.1. Stability of the non-dominant subsystem

Let $V_{L1} : \mathbb{R} \to \mathbb{R}$ be a continuously differentiable, positive definite, common Lyapunov function candidate defined as

$$V_{L1} \triangleq \frac{1}{2} M_1 r_1^2, \tag{24}$$

which satisfies the following inequalities:

$$\frac{c_m}{2} r_1^2 \leq V_{L1} \leq \frac{c_M}{2} r_1^2, \tag{25}$$

where c_m and c_M are introduced in Property 1. To facilitate the subsequent stability analysis, let the following gain conditions apply:

$$k_{1s} > \frac{c_1 + c_{vol}}{k_{min1} c_{b_m}}, \; k_{2s} > \frac{c_2}{k_{min1} c_{b_m}}, \tag{26}$$

$$k_{1e} > \frac{c_{vol} + c_1 + c_2 \Delta_{d1}}{c_{b_e} \Gamma_1}, \; k_{2e} > \frac{c_2}{c_{b_e} \Gamma_1}, \tag{27}$$

where $k_{min1} \in \mathbb{R}_{>0}$ is defined as $k_{min1} \triangleq \min\left(k_{m_l}\right), \forall l \in S, \forall m \in \mathcal{M}$, $\Gamma_1 : \mathbb{R}_{\geq 0} \to \mathbb{R}$ is defined as $\Gamma_1 \triangleq \min\left(1, \gamma_1\right)$, γ_1 is introduced in (6), c_{b_m} is introduced in Property 8, c_{b_e} in Property 9, c_{vol} in Assumption 1, c_1 and c_2 in (12), Δ_{d1} in (10), k_{1s} and k_{2s} in (13), and k_{1e} and k_{2e} in (14).

Theorem 1. *Throughout the assistive mode, when $\dot{q}_1 \leq \dot{q}_{\underline{d}1}$, the closed-loop error system in (15) results in exponential convergence of the cadence on the non-dominant side to $\dot{q}_{\underline{d}1}$, in the sense that*

$$|e_1(t)| \leq \sqrt{\frac{c_M}{c_m}} |e_1\left(t^a_{n,1}\right)| \exp\left[-\frac{\lambda_{a1}}{2}\left(t - t^a_{n,1}\right)\right], \tag{28}$$

$\forall t \in \left[t^a_{n,1}, t^u_{n+1,1}\right)$, $\forall n$, where $\lambda_{a1} : \mathbb{R}_{\geq 0} \to \mathbb{R}_{>0}$ is defined as $\lambda_{a1} \triangleq \frac{2}{c_M}\left[\min\left(c_{b_e} k_{2e}, \; c_{b_m} k_{min1} k_{2s}, \; c_{b_e} \gamma_1 k_{2e}\right) - c_2\right]$, provided the sufficient gain conditions in (26) and (27) are satisfied.

Proof. When $\dot{q}_1 \leq \dot{q}_{\underline{d}1}$; $e_1 = r_1 \geq 0$, $\sigma_{a_1} = 1$, and $\sigma_{r_1} = 0$ (i.e., the non-dominant side subsystem is in the assistive mode and controlled by either FES, the motor, or both). Since B_{M_1} and B_{E_1} are discontinuous, the time derivative of (24) exists almost

everywhere (a.e.) within $t \in \left[t^a_{n,1},\ t^u_{n+1,1}\right)$, $\forall n$, and $\dot{V}_{L1} \overset{a.e.}{\in} \dot{\tilde{V}}_{L1}$ (Kamalapurkar, Rosenfeld, Parikh, Teel, & Dixon, 2019). After substituting (8) and (15), and noting that the FES control input is not saturated when $\sigma_{e_1} = 0$, the derivative of (24) can be solved to yield $\dot{V}_{L1} \overset{a.e.}{\leq} -B_{e_1}\left(k_{1e}|r_1| + k_{2e}r_1^2\right) - \tau_{vol_1}r_1 + \chi_1 r_1$ if $\sigma_{e_1} = 1$, $-\sum_{m\in\mathcal{M}} B_m\sigma_{m_l}k_{m1}\left(k_{1s}r_1 + k_{2s}r_1^2\right) - \tau_{vol_1}r_1 + \chi_1 r_1$ if $\sigma_{e_1} = 0$, $-B_{e_1}\gamma_1\left(k_{1e}|r_1| + k_{2e}r_1^2\right) - \sum_{m\in\mathcal{M}} B_m\sigma_{m_1}\text{sat}_{\beta_{m_1}}\left[k_{m1}\left(k_{1s} + k_{2s}r_1\right)\right]r_1 - \tau_{vol_1}r_1 + \chi_1 r_1$ if $\sigma_{e_1} = \gamma_1$, which can be upper bounded using Properties 7 and 8, Assumption 1, and (12) as

$$\dot{V}_{L1} \overset{a.e.}{\leq} -\left(A - c_{vol} - c_1\right)r_1 - \left(B - c_2\right)r_1^2, \tag{29}$$

which is negative definite in all cases since $r_1 \geq 0$, provided the gain conditions in (26) and (27) are satisfied. In (29), the values of $A : Q \times \mathbb{R}_{>0} \times \mathbb{R}_{\geq 0} \to \mathbb{R}_{>0}$ and $B : Q \times \mathbb{R}_{>0} \times \mathbb{R}_{\geq 0} \to \mathbb{R}_{>0}$ from (29) depend on the switching signals, and are defined as

$$A \triangleq \begin{cases} c_{b_e}k_{1e} & \text{if } \sigma_{e_1} = 1 \\ c_{b_m}k_{min1}k_{1s} & \text{if } \sigma_{e_1} = 0 \\ c_{b_e}\gamma_1 k_{1e} + c_{b_m}\beta_{m1} & \text{if } \sigma_{e_1} = \gamma_1 \end{cases}$$

and

$$B \triangleq \begin{cases} c_{b_e}k_{2e} & \text{if } \sigma_{e_1} = 1 \\ c_{b_m}k_{min1}k_{2s} & \text{if } \sigma_{e_1} = 0 \\ c_{b_e}\gamma_1 k_{2e} & \text{if } \sigma_{e_1} = \gamma_1 \end{cases}.$$

Furthermore, (25) can be used to upper bound (29) as

$$\dot{V}_{L1} \overset{a.e.}{\leq} -\lambda_{a1}V_{L1}, \tag{30}$$

$t \in \left[t^a_{n,1},\ t^u_{n+1,1}\right)$, $\forall n$, where λ_{a1} was defined previously. Solving the inequality in (30), using (25), and performing some algebraic manipulation yields exponential convergence of r_1 and e_1 to zero, as in (28). Since (28) holds for all combinations of σ_{e_1} and σ_{m_1} while $\sigma_{a_1} = 1$, V_{L1} is a common Lyapunov function and the controllers in (13) and (14) are bounded for switching during the assistive mode of the non-dominant side.

Theorem 2. *Throughout the resistive mode, when $\dot{q}_1 \geq \dot{q}_{\underline{d}1}$, the closed-loop error system in (15) results in exponential convergence of the cadence on the non-dominant side to $\dot{q}_{\underline{d}1}$, in the sense that*

$$|r_1(t)| \leq \sqrt{\frac{c_M}{c_m}}\left|r_1\left(t^r_{n,1}\right)\right|\exp\left[-\frac{\lambda_{r1}}{2}\left(t - t^r_{n,1}\right)\right], \tag{31}$$

$\forall t \in \left[t^r_{n,1},\ t^u_{n+1,1}\right)$, $\forall n$, *where $\lambda_{r1} \in \mathbb{R}_{>0}$ is defined as $\lambda_{r1} \triangleq \frac{2}{c_M}\left(c_{b_e}k_{2e} - c_2\right)$, provided the sufficient gain conditions in (27) are satisfied.*

Proof. When $\dot{q}_1 \geq \dot{q}_{\underline{d}1}$; $\sigma_{a_1} = 0$, $\sigma_{r_1} = 1$, and $e_1 + \Delta_{d1} = r_1 \leq 0$ (i.e., the non-dominant side subsystem is in the resistive mode and controlled by the motor). Due to the signum function in (15), the time derivative of (24) exists a.e. within $t \in \left[t^r_{n,1},\ t^u_{n+1,1}\right)$, $\forall n$, and $\dot{V}_{L1} \overset{a.e.}{\in} \dot{\tilde{V}}_{L1}$. After substituting (10) and (15), $\dot{V}_{L1}$ can be upper bounded using Properties 7 and 9, Assumption 1, and (12) as

$$\begin{aligned}\dot{V}_{L1} \overset{a.e.}{\leq}& -\left(c_{b_e}k_{1e} - c_{vol} - c_1 - c_2\Delta_{d1}\right)|r_1| \\ &- \left(c_{b_e}k_{2e} - c_2\right)r_1^2,\end{aligned} \tag{32}$$

$\forall t \in \left[t^r_{n,1},\ t^u_{n+1,1}\right)$, $\forall n$, which is negative definite provided the sufficient gain conditions in (27) are satisfied. Furthermore, (32) can be upper bounded as

$$\dot{V}_{L1} \overset{a.e.}{\leq} -\lambda_{r1}V_{L1}, \tag{33}$$

$\forall t \in \left[t^r_{n,1},\ t^u_{n+1,1}\right)$, $\forall n$, where λ_{r1} was defined previously. Solving (33), rewriting using (25), and performing algebraic manipulation yields (31). Thus, the controllers in (13) and (14) are bounded for switching during the resistive mode of the non-dominant side.

Remark 1. Since the non-dominant side is in the uncontrolled mode when $-\Delta_{d1} < e_1 < 0$, the error is always bounded in the uncontrolled mode. As described in Theorems 1 and 2, $|r_1|$ (which, by (10), is equivalent to e_1 in the assistive mode) decays at an exponential rate in both the assistive and resistive modes to zero. By extension, $|e_1|$ also decays exponentially in the assistive and resistive modes, to values of 0 and Δ_{d1}, respectively. When the non-dominant side enters the resistive mode, the cadence will instantly exponentially decay towards $\dot{q}_{\underline{d}1}$ (i.e., back into the uncontrolled mode), and when entering the assistive mode, the FES and motor controllers on the non-dominant side will ensure the cadence exponentially increases towards $\dot{q}_{\underline{d}1}$. For this particular control objective, there is a desired cadence range, rather than a single value for the desired trajectory, so error convergence to a range (i.e., $[0,\ \Delta_{d1}]$) is desirable, rather than exponential error convergence to zero.

4.2. Stability of the dominant side

Let $V_{L2} : \mathbb{R}^2 \to \mathbb{R}$ be a continuously differentiable, positive definite, common Lyapunov function candidate defined as

$$V_{L2} \triangleq \frac{1}{2}r_2^2 + \frac{1}{2}M_2 r_3^2, \tag{34}$$

which satisfies the following inequalities:

$$\Psi_m\|z\|^2 \leq V_{L2} \leq \Psi_M\|z\|^2, \tag{35}$$

where Ψ_m, $\Psi_M \in \mathbb{R}_{>0}$ are defined as $\Psi_m \triangleq \frac{\min(c_m,\ 1)}{2}$ and $\Psi_M \triangleq \frac{\max(c_M,\ 1)}{2}$, and c_m and c_M are introduced in Property 1. To facilitate the subsequent stability analysis, let the following gain conditions apply

$$k_{4s} > \frac{c_3 + c_{vol}}{c_{b_m}k_{min2}}, k_{5s} > \frac{c_4}{c_{b_m}k_{min2}}, k_{6s} > \frac{c_5}{c_{b_m}k_{min2}}, \tag{36}$$

$$k_{4e} > \frac{c_3 + c_{vol}}{c_{b_e}\Gamma_2}, k_{5e} > \frac{c_4}{c_{b_e}\Gamma_2}, k_{6e} > \frac{c_5}{c_{b_e}\Gamma_2}, \tag{37}$$

where $\Gamma_2 : \mathbb{R} \to \mathbb{R}$ is defined as $\Gamma_2 \triangleq \min(1, \gamma_2)$, γ_2 is introduced in (6), c_{b_m} and c_{b_M} are introduced in Property 8, c_{b_e} in Property 9, c_{vol} in Assumption 1, c_3, c_4, and c_5 in (20), Δ_{d2} in (17), k_{4s}, k_{5s}, and k_{6s} in (21), and k_{4e}, k_{5e}, and k_{6e} in (22).

Theorem 3. *When $q_2 \leq q_{\underline{d}2}$, the closed-loop error system in (23) results in exponential convergence of the position and cadence on the dominant side to $q_{\underline{d}2}$ and $\dot{q}_1$, respectively, in the sense that*

$$\|z(t)\| \leq \sqrt{\frac{\Psi_M}{\Psi_m}}\left\|z\left(t^a_{n,2}\right)\right\|\exp\left(-\frac{\lambda_{a2}}{2}\left(t - t^a_{n,2}\right)\right), \tag{38}$$

$\forall t \in \left[t^a_{n,2},\ t^u_{n+1,2}\right)$, $\forall n$, *where $\lambda_{a2} : \mathbb{R}_{>0} \to \mathbb{R}_{>0}$ is defined as $\lambda_{a2} \triangleq \frac{2\cdot\min\left(c_{b_e}k_{3e},\ c_{b_m}k_{min2}k_{3s},\ c_{b_e}\gamma_2 k_{3e},\ \alpha\right)}{\max(c_M,\ 1)}$, provided the gain conditions in (36) and (37) are satisfied.*

Proof. When $q_2 \leq q_{\underline{d}2}$; $\sigma_{a_2} = 1$, $\sigma_{r_2} = 0$, and $r_2 = e_2 \geq 0$ (i.e., the dominant side subsystem is in the assistive mode and controlled by FES and/or the motor). Similar to the proof of Theorem 1, the time derivative of (34) exists a.e. within $t \in \left[t^a_{n,2},\ t^u_{n+1,2}\right)$, $\forall n$, and $\dot{V}_{L2} \in \dot{\tilde{V}}_{L2}$. After substituting (23), the derivative of (34) can be expressed as $\dot{V}_{L2} \overset{a.e.}{\leq} -B_{e_2}\left[k_{3e}r_3^2 + \left(k_{4e} + k_{5e}\|z\| + k_{6e}\|z\|^2\right)|r_3|\right] + \chi_2 r_3 - \tau_{vol_2}r_3 - \alpha r_2^2$ if $\sigma_{e_2} = 1$, $-\tau_{vol_2}r_3 + \chi_2 r_3 - \alpha r_2^2 - \sum_{m\in\mathcal{M}} B_m\sigma_{m_2}\left[k_{m_2}k_{3s}r_3^2 + k_{m_2}\left(k_{4s} + k_{5s}\|z\| + k_{6s}\|z\|^2\right)|r_3|\right]$ if $\sigma_{e_2} = 0$, $-B_{e_2}\gamma_2\left[\left(k_{4e} + k_{5e}\|z\| + k_{6e}\|z\|^2\right)|r_3| + k_{3e}r_3^2\right] - \tau_{vol_2}r_3 - \alpha r_2^2 - \sum_{m\in\mathcal{M}} B_m\sigma_{m_2}\text{sat}_{\beta_{m_2}}\left[k_{m_2}k_{3s}r_3 + k_{m_2}\left(k_{4s} + k_{5s}\|z\| + k_{6s}\|z\|^2\right)\text{sgn}(r_3)\right]r_3 + \chi_2 r_3$ if $\sigma_{e_2} = \gamma_2$, which can be

upper bounded using Properties 7 and 8, Assumption 1, and (20) as

$$\dot{V}_{L2} \overset{\text{a.e.}}{\leq} -\min\left(c_{b_e}k_{3e},\ c_{b_m}k_{min2}k_{3s},\ c_{b_e}\gamma_2 k_{3e}\right) r_3^2 - \alpha r_2^2, \tag{39}$$

$\forall t \in \left[t^a_{n,2},\ t^u_{n+1,2}\right)$, $\forall n$, provided the gain conditions in (36) and (37) are satisfied. Furthermore, (35) can be used to upper bound (39) as

$$\dot{V}_{L2} \overset{\text{a.e.}}{\leq} -\lambda_{a2} V_{L2}, \tag{40}$$

$\forall t \in \left[t^a_{n,2},\ t^u_{n+1,2}\right)$, $\forall n$, where λ_{a2} was defined previously. The inequality in (40) can be solved and rewritten using (35). Performing some algebraic manipulation yields (38). Since (38) holds for all combinations of σ_{e_2} and σ_{m_2} while $\sigma_{a_2} = 1$, V_{L2} is a common Lyapunov function for switching during the assistive mode of the dominant side (Liberzon, 2003).

Theorem 4. *When $q_2 \geq q_{\underline{d}2}$, the closed-loop error system in (23) results in exponential convergence in the sense that*

$$\|z(t)\| \leq \sqrt{\frac{\Psi_M}{\Psi_m}} \left\|z\left(t^r_{n,2}\right)\right\| \exp\left[-\frac{\lambda_{r2}}{2}\left(t - t^r_{n,2}\right)\right], \tag{41}$$

$\forall t \in \left[t^r_{n,2},\ t^u_{n+1,2}\right)$, $\forall n$, *where $\lambda_{r2} \in \mathbb{R}_{>0}$ is defined as $\lambda_{r2} \triangleq \frac{2\cdot\min\left(c_{b_e}k_{3e},\,\alpha\right)}{\max(c_M,\,1)}$, provided the gain conditions in (37) are satisfied.*

Proof. When $q_2 \leq q_{\underline{d}2}$, then $r_2 \leq 0$, $e_2 \leq 0$, and $\sigma_{r_2} = 1$ (i.e., the cycle-rider system is in the motor-resistance mode). The time derivative of (34) exists a.e. within $t \in \left[t^r_{n,2},\ t^u_{n+1,2}\right)$, $\forall n$, and $\dot{V}_{L2} \in \dot{\tilde{V}}_{L2}$. After substituting (17) and (23), the derivative of (34) can be upper bounded using Properties 7 and 9, Assumption 1, (20), and noting that $r_2 \leq 0$, as

$$\dot{V}_{L2} \overset{\text{a.e.}}{\leq} -c_{b_e}k_{3e}r_3^2 - \alpha r_2^2, \tag{42}$$

which is negative definite provided the gain conditions in (37) are satisfied. Furthermore, since $\dot{V}_{L2} \overset{\text{a.e.}}{\in} \dot{\tilde{V}}_{L2}$, (42) can be upper bounded as

$$\dot{V}_{L2} \leq -\lambda_{r2} V_{L2}, \tag{43}$$

where λ_{r2} is previously defined, and (43) can be solved and rewritten using (35). Algebraic manipulation then yields (41). Since $\|z\| \to 0$, $|r_2|, |r_3| \to 0$.

Remark 2. Since r_2 exponentially decays to zero in both the assistive and resistive modes, (17) can be used to show that e_2 exponentially decays to 0 in the assistive mode and to Δ_{d2} in the resistive mode. The position of the dominant leg exponentially approaches a neighborhood of $\left[q_{\underline{d}2},\ q_{\bar{d}2}\right]$ about a 180 degree offset from the actual position of the non-dominant leg (i.e., q_1), and the cadence of the dominant leg exponentially approaches the cadence of the non-dominant leg.

5. Experiments

To evaluate the performance of the FES and motor controllers in (13), (14), (21), and (22), experiments were conducted on three able-bodied participants and three participants with neurological conditions. Participant N1 was a 25 year old male born with Spina Bifida (L5-S1) and Arnold Chiari Malformation. He was previously active in FES and PT/OT (physical/occupational therapy). Participant N2 was a 64 year old male with Parkinson's disease for 19 years and active in PT/OT, but not FES. Participant N3 was a 52 year old male with drug-induced Secondary Parkinson's Disease for the past year. He was active in neither FES nor PT/OT. The healthy subjects consisted of one female (25 years old) and two males (24 and 26 years old). All participants gave written informed consent approved by the University of Florida Institutional Review Board.

5.1. Split-crank motorized FES-cycling testbed

Similar to the stationary recumbent tricycle (TerraTrike Rover) in Bellman et al. (2017), orthotic boots fixed the rider's feet to the pedals. Each side of the split-crank cycle included an optical encoder (US Digital H1), a 250 Watt 24 V DC brushed electric motor (Unite Motor Co. Ltd.), an ADVANCED Motion Controls[3] (AMC) PS300W24 power supply, and an AMC AB25A100 motor driver. Data acquisition hardware (Quanser Q-PIDe) measured the encoder signals and delivered the motor current. A computer running real-time control software (QUARC, MATLAB/Simulink, Windows 10) at a sampling rate of 500 Hz was used to implement both controllers. The stimulation amplitudes were fixed at 90 mA for the quadriceps and 80 mA for the hamstrings and gluteal muscle groups. The stimulation pulse width for each muscle group was determined by u_{m_l} and u_{s_l} from (4) and (13), respectively, commanded to the current-controlled stimulator (Hasomed RehaStim) by the control software, and delivered to the subjects' muscle groups via self-adhesive, PALS®electrodes[4]. Stimulation frequency was fixed at 60 Hz, as in Bellman et al. (2017) and Eser, Donaldson, Knecht, and Stussi (2003). For safety, an emergency stop switch was attached to the tricycle that enabled participants to stop the stimulation immediately, but no participant found it necessary.

5.2. Protocol

Electrodes were placed over the participant's quadriceps femoris, hamstring, and gluteal muscle groups according to Axelgaard's electrode placement manual[5]. The participant was then seated on the tricycle with their feet secured in the orthotic boots attached to the pedals. The seat position was adjusted so that the subject was comfortable and full knee extension would not occur at any crank position. The position of the participant's lower limbs and seat were measured to calculate the torque transfer ratios, which establish the switching signals in the assistance mode, as in Bellman et al. (2017). To avoid large initial errors, the motor tracked a linear cadence increasing from zero to $\dot{q}_{\underline{d}1}$ before the developed control scheme was implemented for the remaining 120 s. Participants were asked to contribute volitionally while the FES and motor controllers for each side were implemented to maintain a cadence within the desired cadence and phase shift regions. A significant challenge with the split-crank cycle is to build momentum and sustain a pedaling motion. For comparison and to demonstrate the significance of the controllers on a split-crank cycle, able-bodied participants were asked to perform a separate trial (random order) where they attempted to remain in the desired bounds with only volitional input and no input from the controllers; however, one able-bodied participant was unable to initiate continuous pedaling on the split-crank cycle. For all participants, the right leg was treated as the non-dominant side and tracked the desired cadence range, while the left leg was treated as the dominant side and tracked the position offset (and hence, cadence) from the right side. The participant was able to view the real-time cadence of the non-dominant side in relation to the upper and lower thresholds, as in the top left plot in Figs. 1 and 2. The minimum desired crank velocity $\dot{q}_{\underline{d}1}$ was defined as $\dot{q}_{\underline{d}1} \triangleq \frac{5\pi}{3}$ rad/s and the velocity range Δ_{d1} was defined as $\Delta_{d1} \triangleq \frac{\pi}{3}$ rad/s for participants with neurological conditions and $\Delta_{d1} \triangleq \frac{\pi}{6}$ rad/s for able-bodied participants to increase the

[3] ADVANCED Motion Controls supported the development of this testbed by providing discounts on their branded items.

[4] Surface electrodes were provided compliments of Axelgaard Manufacturing Co., Ltd.

[5] http://www.palsclinicalsupport.com/videoElements/ videoPage.php.

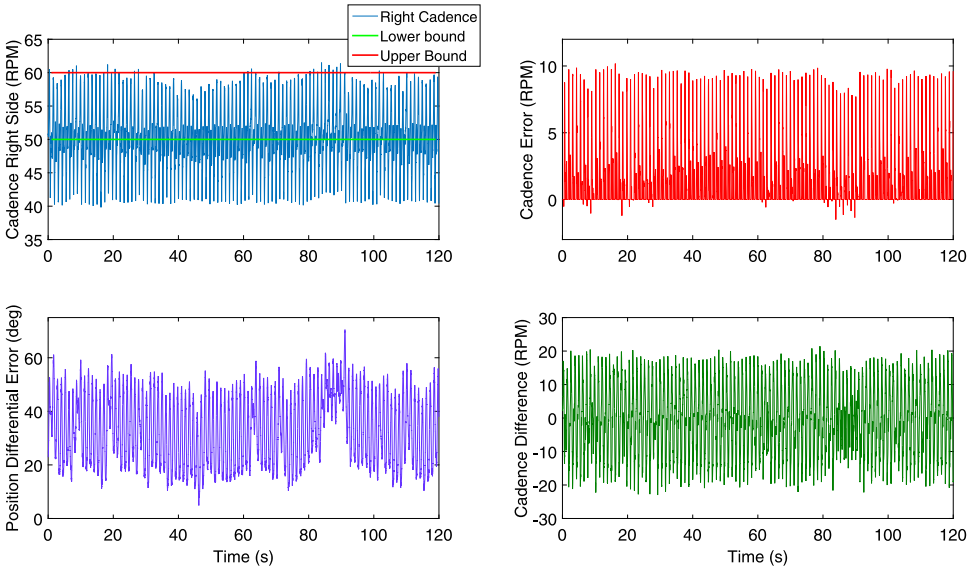

Fig. 1. FES cycling data for Participant N3. (Top left) The right leg cycling cadence compared to the upper and lower bounds on the desired cadence region; (top right) right leg cadence error; (bottom left) left leg position error; and (bottom right) the cadence differential between the two sides.

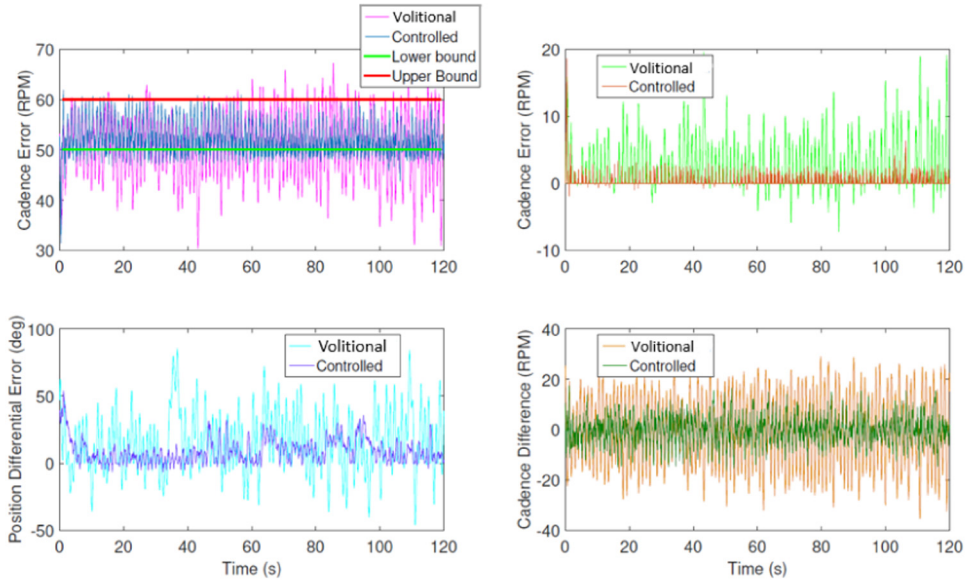

Fig. 2. FES cycling data for Participant C4/V4 during both the controlled and volitional trials. (Top left) The right leg cycling cadence compared to the upper and lower bounds on the desired cadence region; (top right) right leg cadence error; (bottom left) left leg position error; and (bottom right) the cadence differential between the two sides.

difficulty level. The desired crank position and position range for the non-dominant leg were defined as $q_{d2} \triangleq q_1 - \pi - \Delta_{d2}/2$ rad and $\Delta_{d2} \triangleq \frac{\pi}{36}$ rad. The control gains were selected within the following ranges: $k_{1e} \in [1, 4]$, $k_{2e} \in [7.5, 20]$, $k_{3e} \in [2, 2.4]$, $k_{4e} \in [3, 3.6]$, $k_{5e} \in [2, 2.4]$, $k_{6e} \in [8, 9.6]$, $k_{1s} \in [20, 26.4]$, $k_{2s} \in [18, 21.6]$, $k_{3s} \in [12, 15]$, $k_{4s} \in [15, 18]$, $k_{5s} \in [1, 2]$, $k_{6s} \in [1, 3]$, $\alpha = 1$.

5.3. Results

Figs. 1 and 2 depict performance data for neurological participant N3 and control participant C4 from two minutes of split-crank cycling with intermittent FES and motor inputs to the volitionally pedaling participants. Data from the volitional trials are overlayed for the two participants that completed the volitional trial. Position and cadence errors from the left and right legs, respectively, are listed in Table 1 for the controlled and volitional trials, along with the cadence differential between the two legs. Errors are calculated and plotted as the difference between the lower bound and the actual position/cadence when below the desired range, the difference between the upper bound and the actual position/cadence when above the desired range, and equal to zero when pedaling anywhere between the lower and upper state bounds. Figs. 3 and 4 display both the FES control inputs to the muscle groups as well as the motor control inputs to each side for participants N3 and C4.

6. Discussion

The controller for each side switched between three modes based on velocity for the right side and position for the left

Table 1
Performance metrics from the volitional and controlled trials.

Participant/Trial[a]	Cadence error, right leg (RMS (avg. ± std. dev.), RPM)	Position error, left leg (RMS (avg. ± std. dev.), deg)	Cadence differential (RMS (avg. ± std. dev.), RPM)
N1	2.84 (1.35 ± 2.50)	13.50 (8.96 ± 10.10)	10.43 (−0.04 ± 10.43)
N2	4.32 (−1.20 ± 4.15)	16.44 (3.23 ± 16.12)	16.25 (−0.16 ± 16.25)
N3	3.16 (−1.73 ± 2.65)	36.04 (−33.55 ± 13.16)	2.56 (−1.78 ± 1.84)
Mean of N trials	3.44 (0.27 ± 3.19)	21.99 (−9.27 ± 13.35)	11.22 (−0.67 ± 11.20)
C4	1.00 (−0.30 ± 0.95)	12.63 (−8.89 ± 8.97)	5.29 (−0.13 ± 5.29)
C5	3.65 (−1.49 ± 3.34)	8.56 (−2.63 ± 8.15)	8.76 (−0.27 ± 8.76)
C6[b]	2.43 (−0.83 ± 2.28)	13.06 (−9.28 ± 9.19)	7.65 (−0.06 ± 7.65)
Mean of C trials	2.36 (−0.87 ± 2.40)	11.42 (−6.93 ± 8.78)	7.38 (−0.15 ± 7.38)
V4	4.21 (−2.11 ± 3.64)	26.71 (−15.12 ± 22.02)	13.92 (−0.17 ± 13.92)
V5	13.86 (−7.20 ± 11.84)	45.42 (21.24 ± 40.15)	20.64 (−0.29 ± 20.64)
Mean of V trials	9.92 (−4.66 ± 8.76)	32.95 (6.12 ± 32.38)	17.60 (−0.23 ± 17.60)

[a]N refers to participants with neurological conditions. C refers to controlled trials with able-bodied participants. V refers to completely volitional trials with able-bodied participants.
[b]Participant C6 was unable to pedal the split-crank cycle volitionally.

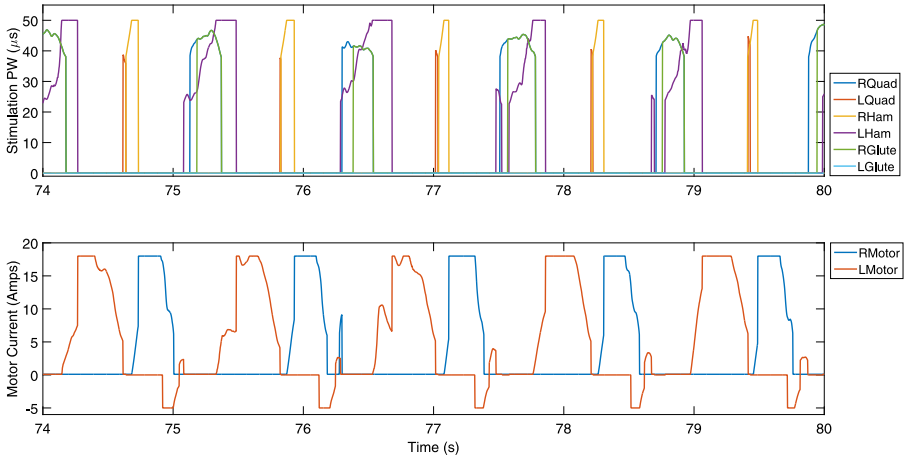

Fig. 3. (Top) FES control input, saturated at 50 μs, and (bottom) motor control inputs for seconds 74–80 of Trial N3. For better resolution and understanding, the plots are magnified to show six seconds, or approximately five crank cycles that encompass the pattern seen throughout the trial. The motors are active with a positive current in the non-FES regions and when the FES controller saturates, and active with a negative current in the resistive mode.

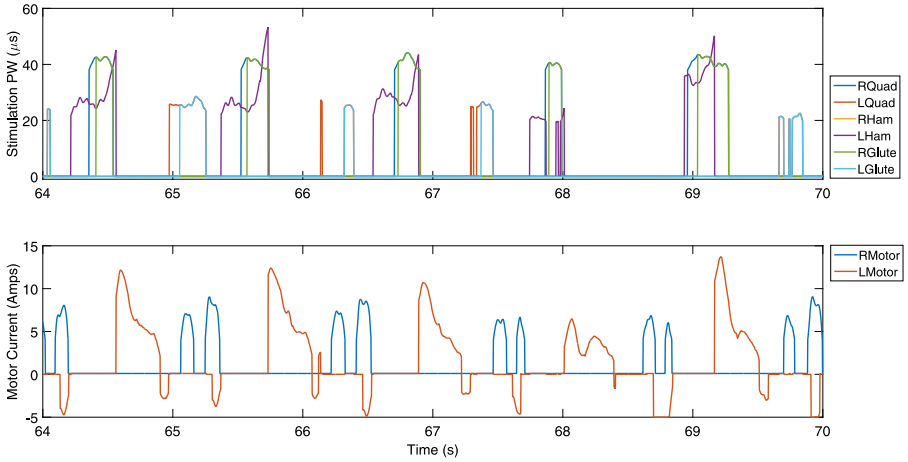

Fig. 4. (Top) FES control input and (bottom) motor control inputs for Trial C4. For better resolution and understanding, the plots are magnified to show six seconds, or approximately five crank cycles that encompass the pattern seen throughout the trial.

side. When the right or left side was in the assistive mode, the corresponding control input switched between FES and the motor. When in the resistive mode, a negative control input was provided to the motor on the corresponding side. In the uncontrolled mode, no control input was provided by FES or the motor for that side.

When pedaling on a split-crank cycle, the gravitational torques on the right and left legs do not balance each other like they do when pedaling a single-crank cycle. At points of the crank cycle where one leg is accelerated by gravity, the other decelerates, accounting for the larger position and cadence errors and standard deviations compared to other FES-cycling studies (Bellman et al., 2017). However, the performance of the three mode controller with FES saturation significantly improved upon the performance achieved when pedaling without FES and motor contribution, as seen in the volitional trial results in Table 1. Moreover, one able-bodied participant (C6) could not achieve a cycling motion by pedaling volitionally without contribution from the developed controllers. Thus, the volitional for participant C6 trial was stopped.

As seen in Table 1, standard deviations on the left side were greater than those of the right side. The greater variance is due to the right side tracking a constant cadence range and the left side tracking a range based around the moving right side. Moreover, it was difficult for participants to monitor their performance with respect to the bounds on both the right and left sides. Instead, the participant was asked to watch their cadence performance on the right side and attempt to maintain a proper phase shift of 180 degrees.

All six controlled results display a similar pattern. Since larger forces are required to rotate the crank through the portion of the crank cycle corresponding to hamstring activation (i.e., the "upward" motion), the control inputs (shown in Figs. 3 and 4) and errors (Figs. 1 and 2) are greater in those regions than in other regions of the crank cycle. For all participants, the cadence slowed and lagged the opposing leg when in the hamstring region. On the contrary, gravitational forces caused each leg to accelerate during the "downward" portion of the crank cycle where the quadriceps are used to extend the legs. During this portion of the crank cycle, the leg typically entered the uncontrolled or resistive mode, whether or not the volitional contribution was large. If the right leg's cadence is larger than the upper cadence bound or the left leg passes the upper position bound, then the respective motor applies a negative (i.e., resistive) control input, pushing the leg back into the desired uncontrolled mode. While the stability analysis ensures immediate transition back into the uncontrolled mode after crossing a cadence bound, the cadence and position errors deviate outside the desired region for all participants, particularly during regions of opposing gravitational force. Gain tuning in favor of a higher control input at the bounds could limit these deviations; however, a strong immediate force may feel unnatural to the rider and unmodeled dynamics from human reaction may introduce further problems. Moreover, in Participant N3, the maximum motor control output was reached, so increasing the gains would not have better constrained pedaling to the desired regions. The size of the desired uncontrolled regions affects the error values since time spent in the desired region is characterized by an error of zero. Moreover, modeling the rider's impulse reactions to stronger forces upon crossing the boundaries is an open problem.

While the results for the participants display many similarities, there were also notable difference. For example, the FES input saturated more often for participants with neurological impairments since they may necessitate higher stimulation and/or have hypersensitivity (and thus, a lower comfort threshold). Because Participant N1 had a comfort threshold of 60 μs, the FES controller saturated most often for him. With FES input saturation, additional input was distributed to the motor.

Participant N2 had a comfort threshold of 95 μs. The FES controller saturated in the right and left hamstring regions, which aligns with the greater force required to lift the leg through that portion of the crank cycle. The control input to the right quadriceps also saturated, but less frequently than the hamstrings. To maintain full control authority when the FES saturates, the motor is also activated according to (5), yielding a cyclic pattern in the motor control input.

Participant N3 chose the lowest comfort threshold of 50 μs, yet muscle contractions were visible. Due to Participant N3's mobility and sitting position, both of his legs required more force than the others to rotate the crank during hamstring activation. Even with volitional contribution, the FES controller saturated in both hamstring regions nearly every cycle, as seen in the top plot of Fig. 3. Theoretically, the system can handle an unlimited control input by distributing the remainder to the corresponding motor, such as the scenario with Participants N1 and N2. However, the motor control input was saturated for safety and physical limitation. For Participant N3, both the FES and the motor control inputs saturated.

Participant C4 completed a volitional-only experiment (V4 in Table 1) and an experiment with motor and FES control implemented. Using only volition, the participant aimed to keep errors within the respective desired regions for both legs. Fig. 2 displays the cadence over time and cadence and position errors for both the controlled and volitional trials. Compared to volitional pedaling, Table 1 indicates that all average errors were significantly improved when the controller was implemented. RMS errors improved by 76.3% from 4.20 RPM to 1.00 RPM, 52.7% from 26.71 degrees to 12.63 degrees, and 62.0% from 13.92 RPM to 5.29 RPM for the right cadence error, left position error, and cadence differential between the right and left.

Participant C5 also completed a volitional-only trial (V5 in Table 1). The cadence and position errors and cadence differential improved with the three mode controller by 73.6% from 13.86 RPM to 3.66 RPM, 81.1% from 45.42 degrees to 8.56 degrees, and 57.5% from 20.64 RPM to 8.76 RPM, respectively.

Participant C6 was unable to consistently pedal the split-crank cycle using only volitional input. While there is no volitional data to compare to the controlled data, the inability of the able-bodied participant to pedal volitionally on the split-crank cycle highlights the benefit of the controller, particularly when the leg's motion is opposing gravitational forces.

In Rouse et al. (2020) by the authors, nine stroke patients pedaled according to a similar three mode protocol, aiming only for a desired cadence range on a single-crank tricycle. The average percentage of time spent in the desired cadence region was 50.48%. Here, the average percentage of time spent in the desired cadence region on the right side was 40.8% for participants with a neurological condition and a comparable 49.4% for able-bodied participants.

As seen in Table 1, the right cadence errors, left position errors, and cadence differentials averaged across all participants with neurological conditions were higher than those of healthy participants with the three mode controller implemented, but lower than those of healthy participants pedaling with only volitional input.

7. Conclusion

The development in this paper provides a control strategy for a combination of FES and motor inputs to enable a volitionally contributing rider of a split-crank cycle to maintain a cadence within a desired range, as well as a phase shift between the two

legs within a desired region centered around 180 degrees. Despite unknown disturbances and arbitrary switching, a Lyapunov-like analysis proved exponential convergence to the desired cadence range (i.e., $e_1 \in [0,\ \Delta_{d1}]$) on the non-dominant side and position range (i.e., $e_2 \in [0,\ \Delta_{d2}]$) on the dominant side. Experiments on healthy participants and participants with neurological conditions validated the use of the control system in all three modes for people with a broad range of abilities to pedal a tricycle decoupled at the crank within a desired range. The developed control system has the potential to advance established FES-cycling protocols for movement disorder rehabilitation exercises. The strategy in this paper presents a way of addressing the asymmetries associated with numerous movement disorders such as stroke or a neurological injury to just one side of the body. However, using the FES and motor controllers, a wide range of volitional abilities could be accommodated, such that any rider could pedal within desired cadence and position offset ranges.

Acknowledgments

This research is supported in part by Natioal Science Foundation, USA award numbers DGE-1842473 and 1762829. Any opinions, findings and conclusions, or recommendations expressed in this material are those of the author(s) and do not necessarily reflect the views of the sponsoring agency.

References

Ambrosini, E., Ferrante, S., Ferrigno, G., Molteni, F., & Pedrocchi, A. (2012). Cycling induced by electrical stimulation improves muscle activation and symmetry during pedaling in hemiparetic patients. *IEEE Transactions on Neural Systems Rehabilitation Engineering*, *20*(3), 320–330.

Ambrosini, E., Ferrante, S., Pedrocchi, A., Ferrigno, G., & Molteni, F. (2011). Cycling induced by electrical stimulation improves motor recovery in postacute hemiparetic patients: A randomized controlled trial. *Stroke*, *42*(4), 1068–1073.

Ambrosini, E., Ferrante, S., Schauer, T., Ferrigno, G., Molteni, F., & Pedrocchi, A. (2014). An automatic identification procedure to promote the use of FES-cycling training for hemiparetic patients. *Journal of Healthcare Engineering*, *5*(3), 275–292.

Asl, H. J., Narikiyo, T., & Kawanishi, M. (2017). An assist-as-needed control scheme for robot-assisted rehabilitation. In *2017 American control conference* (pp. 198–203).

Banala, S., Kim, S., Agrawal, S., & Scholz, J. (2009). Robot assisted gait training with active leg exoskeleton (ALEX). *IEEE Transactions on Neural Systems and Rehabilitation Engineering*, *17*(1), 2–8.

Bellman, M. J., Cheng, T.-H., Downey, R. J., & Dixon, W. E. (2014). Stationary cycling induced by switched functional electrical stimulation control. In *Proc. Am. control conf.* (pp. 4802–4809).

Bellman, M. J., Downey, R. J., Parikh, A., & Dixon, W. E. (2017). Automatic control of cycling induced by functional electrical stimulation with electric motor assistance. *IEEE Transactions on Automation Science and Engineering*, *14*(2), 1225–1234.

Chen, H., Chen, S., Chen, J., Fu, L., & Wang, Y. (2005). Kinesiological and kinematical analysis for stroke subjects with asasymmetric cycling movement patterns. *Journal of Electromyography & Kinesiology*, *15*(6), 587–595.

Cousin, C. A., Duenas, V., Rouse, C., & Dixon, W. E. (2018). Admittance control of motorized functional electrical stimulation cycle. In *Proc. IFAC conf. cyber. phys. hum. syst.* (pp. 328–333).

Duschau-Wicke, von Zitzewitz, J., Caprez, A., Lunenburger, L., & Riener, R. (2010). Path control: a method for patient-cooperative robot-aided gait rehabilitation. *IEEE Transactions on Neural Systems and Rehabilitation Engineering*, *18*(1), 38–48.

Eser, P. C., Donaldson, N., Knecht, H., & Stussi, E. (2003). Influence of different stimulation frequencies on power output and fatigue during FES-cycling in recently injured SCI people. *IEEE Transactions on Neural Systems and Rehabilitation Engineering*, *11*(3), 236–240.

Estay, F. I. E., Rouse, C., Cohen, M., Cousin, C., & Dixon, W. E. (2019). Cadence and position tracking for decoupled legs during switched split-crank motorized FES-cycling. In *Proc. Am. control conf.* (pp. 854–859).

Ferrante, S., Pedrocchi, A., Ferrigno, G., & Molteni, F. (2008). Cycling induced by functional electrical stimulation improves the muscular strength and the motor control of individuals with post-acute stroke. *European Journal of Physical and Rehabilitation Medicine*, *44*(2), 159–167.

Hogan, N., Krebs, H. I., Rohrer, B., Palazzolo, J., Dipietro, L., Faoli, S., et al. (2006). Motions or muscles? Some behavioral factors underlying robotic assistance or motor recovery. *Journal of Rehabilitation Research and Development*, *43*(5), 605–618.

Hooker, S. P., Figoni, S. F., Rodgers, M. M., Glaser, R. M., Mathews, T., Suryaprasad, A. G., et al. (1992). Physiologic effects of electrical stimulation leg cycle exercise training in spinal cord injured persons. *Archives of Physical Medicine and Rehabilitation*, *73*(5), 470–476.

Idsø, E. S., Johansen, T., & Hunt, K. J. (2004). Finding the metabolically optimal stimulation pattern for FES-cycling. In *Proc. conf. of the int. funct. electrical stimulation soc.* Bournemouth, UK.

Iyanaga, T., Abe, H., Oka, T., Miura, T., Iwasaki, R., Takase, M., et al. (2019). Recumbent cycling with integrated volitional control electrical stimulation improves gait speed during the recovery stage in stroke patients. *Journal of Exercise Rehabilitation*, *15*(1), 95–102.

Janssen, T. W., Beltman, M., Elich, P., Koppe, P. A., Konijnenbelt, H., de Haan, A., et al. (2008). Effects of electric stimulation-assisted cycling training in people with chronic stroke. *Archives of Physical Medicine and Rehabilitation*, *89*(3), 463–469.

Johnston, T., Smith, B., Oladeji, O., Betz, R., & Lauer, R. (2008). Outcomes of a home cycling program using functional electrical stimulation or passive motion for children with spinal cord injury: a case series. *The Journal of Spinal Cord Medicine*, *31*(2), 215–221.

Kamalapurkar, R., Rosenfeld, J. A., Parikh, A., Teel, A. R., & Dixon, W. E. (2019). Invariance-like results for nonautonomous switched systems. *IEEE Transactions on Automatic Control*, *64*(2), 614–627.

Kraft, G., Fitts, S., & Hammond, M. (1992). Techniques to improve function of the arm and hand in chronic hemiplegia. *Archives of Physical Medicine and Rehabilitation*, *73*(3), 220–227.

Kuhn, D., Leichtfried, V., & Schobersberger, W. (2014). Four weeks of functional electrical stimulated cycling after spinal cord injury: a clinical Study. *The International Journal of Rehabilitation Research*, *37*, 243–250.

Liberzon, D. (2003). *Switching in systems and control*. Birkhauser.

Van der Loos, M., Worthen-Chaudhari, L., & Schwandt, D. (2010). A split-crank bicycle ergometer uses servomotors to provide programmable pedal forces for studies in human biomechanics. *IEEE Transactions on Neural Systems Rehabilitation Engineering*, *18*(4), 445–452.

Pehlivan, A. U., Losey, D. P., & O'Malley, M. K. (2016). Minimal assist-as-needed controller for upper limb robotic rehabilitation. *IEEE Transactions on Robotics*, *32*(1), 113–124.

Rouse, C., Cousin, C., Allen, B. C., & Dixon, W. E. (2019). Split-crank cadence tracking for switched motorized FES-cycling with volitional pedaling. In *Proc. Am. control conf.* (pp. 4393–4398).

Rouse, C., Cousin, C., Duenas, V. H., & Dixon, W. E. (2017). Switched motorized assistance during switched functional electrical stimulation of the biceps brachii to compensate for fatigue. In *IEEE conf. dec. control.* (pp. 5912–5918).

Rouse, C., Cousin, C., Duenas, V. H., & Dixon, W. E. (2018). Cadence tracking for switched FES cycling combined with voluntary pedaling and motor resistance. In *Proc. Am. control conf.* (pp. 4558–4563).

Rouse, C., Downey, R., Gregory, C., Cousin, C., Duenas, V., & Dixon, W. E. (2020). FES cycling in stroke: Novel closed-loop algorithm accommodates differences in functional impairments. *IEEE Transactions on Biomedical Engineering*, *67*(3), 738–749.

Sadowsky, C. L., Hammond, E. R., Strohl, A. B., Commean, P. K., Eby, S. A., Damiano, D. L., et al. (2013). Lower extremity functional electrical stimulation cycling promotes physical and functional recovery in chronic spinal cord injury. *The Journal of Spinal Cord Medicine*, *36*(6), 623–631.

Srivastava, S., Kao, P., Kim, S., Stegall, P., Zanotto, D., Higginson, J., et al. (2015). Assist-as-needed robot-aided gait training improve walking function in individuals following stroke. *IEEE Transactions on Neural Systems and Rehabilitation Engineering*, *23*(6), 956–963.

Srivastava, S., Kao, P., Reisman, D., Scholz, J., Argrawal, S., & Higginson, J. (2016). Robotic assist-as-needed as an alternative to therapist-assisted gait rehabilitation. *International Journal of Physical Medicine & Rehabilitation*, *4*(5), 370.

Ting, L., Kautz, S., Brown, D., Van der Loos, H., & Zajac, F. E. (1998). Bilateral integration of sensorimotor signals during pedaling. *Annals of the New York Academy of Sciences*, *860*(1), 513–516.

Ting, L., Kautz, S., Brown, D., & Zajac, F. (2000). Contralateral movement and extensor force generation alter flexion phase muscle coordination in pedaling. *Journal of Neurophysiology*, *83*(6), 3351–3365.

Ting, L., Raasch, C. C., Brown, D., Kautz, S., & Zajac, F. E. (1998). Sensorimotor state of the contralateral leg affects ipsilateral muscle coordination of pedaling. *Journal of Neurophysiology*, *80*(3), 1341–1351.

Courtney A. Rouse, Ph.D., received her doctorate degree in mechanical engineering from the University of Florida in 2019. Her dissertation, which earned the 2020 Best Dissertation Award in Mechanical and Aerospace Engineering, focused on control of motorized functional electrical stimulation exercises for neuromuscular therapy. She now works as a research engineer in the Intelligent Systems division at Southwest Research Institute.

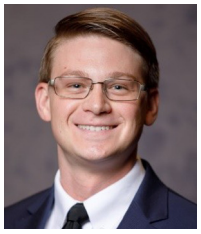

Dr. Christian A. Cousin joined the Department of Mechanical Engineering at The University of Alabama as a faculty member in July 2019 after graduating with his doctorate from the University of Florida. He was awarded a National Science Foundation Graduate Research Fellowship in the spring of 2016 and his research interests include nonlinear and adaptive control, switched and hybrid systems, cyber–physical systems, hybrid exoskeletons, functional electrical stimulation, human–robot interaction, rehabilitation, and machine learning.

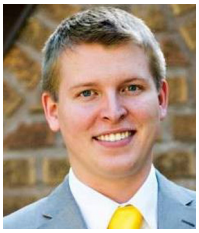

Brendon C. Allen received his Bachelor of Science degree in Mechanical Engineering in December 2015 from the University of Florida and his Master of Science degree in Mechanical Engineering in 2018 from Brigham Young University, Provo. He is currently pursuing a Ph.D. degree in Mechanical Engineering with a focus on nonlinear controls under the supervision of Dr. Warren Dixon.

Warren E. Dixon received his Ph.D. in 2000 from the Department of Electrical and Computer Engineering, Clemson University. He was selected as a Eugene P. Wigner Fellow and worked as a staff researcher at Oak Ridge National Laboratory. In 2004, he joined the University of Florida in the Mechanical and Aerospace Engineering Department, where he currently holds the Newton C. Ebaugh Professorship. His main research interest has been the development and application of Lyapunov-based control techniques for uncertain nonlinear systems. His work has been acknowledged by various career and best paper awards, and he attained ASME and IEEE Fellow for contributions to adaptive control of uncertain nonlinear systems.